fermentation

MDPI

Article

Co-Cultivation Enhances Extracellular Endoglucanase Activity in Two Insect-Gut-Derived *Bacillus* Isolates

Wanting Xia [1,2], Li Fang [1], Fangmin Chen [1,2,*], Xinqi Ji [1], Simiao Li [1] and Xinyao Yang [2]

[1] Liaoning Province Key Laboratory of Urban Integrated Pest Management and Ecological Security, College of Life Science and Bioengineering, Shenyang University, Shenyang 110044, China; wantingxia1998@163.com (W.X.); 15041504181@163.com (L.F.); 15141848133@163.com (X.J.); 18698245027@163.com (S.L.)

[2] Key Laboratory of Ecological Restoration of Regional Contaminated Environment, Ministry of Education, Shenyang University, Shenyang 110044, China; xinyao.yang@syu.edu.cn

* Correspondence: fangminchen@syu.edu.cn

Abstract

Insect guts harbor microorganisms with carbohydrate-active enzymes, yet their potential as enzyme-production strains and the benefits of co-cultivation remain insufficiently characterized. In this study, 180 bacterial isolates from nine insect species were screened for carboxymethyl cellulose (CMC)-hydrolyzing activity. Two non-hemolytic isolates, H11 and Q5-3, were assigned to the genus *Bacillus* based on morphological characteristics and 16S rRNA gene analysis. Their initial extracellular endoglucanase activities were 156.67 ± 4.17 and 190.36 ± 4.29 U/mL, respectively, and increased to 228.01 ± 2.73 and 283.28 ± 2.06 U/mL after orthogonal array optimization. Central composite design predicted a maximum volumetric activity of 340.81 U/mL at approximately 16% (*v*/*v*) total inoculum and a Q5-3/H11 inoculum ratio of 2.08; independent validation yielded 339.17 ± 3.97 U/mL. Additional H11 and Q5-3 monoculture controls evaluated at the same total inoculum proportion showed lower mean volumetric activities than the validated co-culture. PCR screening produced expected-size amplicons for five putative endoglucanase-related targets in both isolates. These results indicate that H11 and Q5-3 are promising insect-gut-derived candidates for extracellular endoglucanase production and that co-cultivation can enhance volumetric enzyme activity on CMC without genetic modification. This study establishes candidate strains and a validated co-cultivation process in a controlled soluble-CMC model system, providing a process-development basis for subsequent evaluation of strain interactions and performance on insoluble cellulose and representative lignocellulosic substrates.

Keywords: insect gut bacteria; *Bacillus*; carboxymethyl cellulose; endoglucanase; co-cultivation

Check for updates

Academic Editor: Penka Petrova

Received: 29 July 2026
Revised: 21 September 2026
Accepted: 14 October 2026
Published: 16 October 2026

Copyright: © 2026 by the authors. Licensee MDPI, Basel, Switzerland. This article is an open access article distributed under the terms and conditions of the Creative Commons Attribution (CC BY) license.

1. Introduction

Insects are among the most abundant and diverse arthropods and play important roles in ecosystem functioning [1]. In phytophagous insects, the continuous ingestion of plant tissues rich in cellulose and other structural polysaccharides creates a strong nutritional pressure for efficient carbohydrate utilization [2]. Their guts therefore constitute dynamic and functionally selective microecosystems in which host physiology, diet, and associated microorganisms interact. Gut microorganisms can influence host nutrition, metabolism, and immunity through colonization and the production of metabolites and extracellular enzymes, whereas the host shapes microbial composition through physicochemical barriers

and bioactive compounds [3,4]. Under these diet-driven selective conditions, bacteria capable of producing carbohydrate-active enzymes may be preferentially maintained because they can contribute to the breakdown of plant-derived polysaccharides and improve nutrient accessibility [5,6]. Consequently, the guts of phytophagous insects represent a biologically targeted reservoir for isolating extracellular cellulolytic bacteria with potential value for cellulase production and lignocellulosic bioprocess development.

Recent studies have demonstrated that insect digestive tracts harbor cellulolytic bacteria and microbial consortia across diverse host groups. Active cellulolytic isolates have been recovered from cotton bollworm larvae [7], termites [8,9], grasshoppers [10], cerambycid larvae [11], and white grubs [12], while ex vivo bioreactor studies have further shown that gut-derived microbial consortia from phytophagous and xylophagous insects can retain lignocellulose-transforming activity outside the host [13]. Together, these findings support insect guts as functionally enriched sources of cellulase-producing microorganisms. However, much of the culture-based research has focused on individual isolates, although extracellular polysaccharide conversion in microbial communities may involve strains with different enzyme repertoires and metabolic capacities. Co-cultivation therefore provides a practical approach for integrating complementary microbial functions, improving substrate utilization, and potentially increasing volumetric cellulolytic enzyme activity without genetic modification. Previous studies have reported enhanced cellulolytic enzyme production or improved lignocellulosic substrate conversion in bacterial and fungal mixed-culture systems [14,15]. These findings provide a rationale for evaluating co-cultivation as a practical approach to improve extracellular cellulase production by insect-gut-derived bacterial isolates.

Cellulose is one of the most abundant renewable polysaccharides and represents an important feedstock for sustainable bioprocessing and the valorization of agricultural residues [16,17]. Its enzymatic conversion depends on the coordinated action of endoglucanases, exoglucanases, and β-glucosidases, among which endoglucanases initiate hydrolysis by cleaving internal β-1,4-glycosidic bonds and increasing substrate accessibility for subsequent enzymatic reactions [18,19]. Carboxymethyl cellulose is commonly used as a model carbon source for screening cellulase-producing microorganisms and evaluating extracellular endoglucanase production because of its solubility and experimental reproducibility. Therefore, identifying efficient enzyme-producing strains and developing cultivation strategies that enhance extracellular endoglucanase activity are important steps toward constructing more effective microbial systems for lignocellulosic bioprocessing.

Improving cellulase biotechnology requires both efficient microbial producers and cultivation strategies that increase enzyme titres in a simple and scalable manner. In this study, insect-gut bacteria were screened as a targeted source of cellulolytic microorganisms, leading to the selection of two insect-gut-derived *Bacillus* isolates, H11 and Q5-3, with strong extracellular endoglucanase activity. Their enzyme-production performance was optimized under monoculture and co-cultivation conditions to evaluate whether a mixed-strain process could further improve volumetric endoglucanase output without genetic modification. By integrating ecological bioprospecting with fermentation optimization, this work provides candidate production strains and a process-development framework for future cellulase production and the valorization of cellulose-rich agricultural residues.

2. Materials and Methods

2.1. Primary Screening of CMC-Hydrolyzing Bacterial Isolates

An established collection of 180 purified bacterial isolates obtained from the intestinal tracts of nine wild insect species collected at multiple locations in Shenyang, Liaoning Province, China, was used for primary screening. The collection included *Lucilia sericata*,

Apis cerana, *Locusta migratoria manilensis*, *Shirakiacris shirakii*, *Atractomorpha lata*, *Vespa affinis*, *Gryllus testaceus*, *Camponotus japonicus*, and *Atractomorpha sinensis*, representing multiple feeding guilds. Unless otherwise stated, routine chemical reagents used in this study were purchased from Beijing Dingguo Changsheng Biotechnology Co., Ltd. (Beijing, China). Sodium carboxymethyl cellulose (CMC-Na; Shanghai Macklin Biochemical Technology Co., Ltd., Shanghai, China; catalog no. C804625,) was used as the screening substrate. The CMC agar medium contained 7.5 g/L CMC-Na, 3.0 g/L peptone, 0.5 g/L yeast extract, 2.0 g/L KH_2PO_4, 0.3 g/L $MgSO_4 \cdot 7H_2O$, 0.3 g/L $CaCl_2$, and 20.0 g/L agar, with the initial pH adjusted to 7.0. A purified colony of each isolate was picked with a sterile toothpick and spot-inoculated onto the CMC agar plates. After incubation at 37 °C for 72 h, the plates were flooded with 0.1% (*w*/*v*) Congo red solution and stained for 15 min. The staining solution was removed, and the plates were rinsed with distilled water and subsequently destained with 5% (*w*/*v*) NaCl for 20 min. The diameter of the hydrolysis zone (*D*) and colony diameter (*d*) were measured, and the *D*/*d* ratio was calculated. Isolates with $D/d > 3.0$ were selected for subsequent quantitative determination of extracellular endoglucanase activity.

2.2. Preparation of Crude Extracellular Enzyme and Endoglucanase Assay

For crude extracellular enzyme production, the isolates were cultivated in a liquid CMC-containing medium with the same composition as the CMC screening agar medium described above, except that agar was omitted. Following cultivation, the bacterial cultures were centrifuged at 10,000× *g* for 5 min at 4 °C, and the clarified culture supernatants were collected as crude extracellular enzyme preparations. Extracellular endoglucanase activity was estimated as carboxymethyl cellulase (CMCase) activity using CMC-Na as the substrate, based on the DNS assay described by McKee [20]. The reaction mixture contained 0.5 mL of 1% (*w*/*v*) CMC-Na prepared in 50 mM sodium phosphate buffer (pH 7.0) and 0.5 mL of the clarified culture supernatant. After incubation at 50 °C for 30 min, the reaction was terminated by adding 1.5 mL of DNS reagent (Phygene Biotechnology Co., Ltd., Fuzhou, China), followed by heating in a boiling-water bath for 5 min. After cooling to room temperature, absorbance was measured at 540 nm using an Infinite 200 PRO microplate reader (Tecan Group Ltd., Männedorf, Switzerland). A matched supernatant/enzyme blank was prepared for each sample using the same volumes of CMC substrate and culture supernatant as in the reaction mixture. For the blank, DNS reagent was added before the incubation step to terminate enzyme activity and thereby prevent hydrolysis of CMC. The blank was subsequently subjected to the same boiling and absorbance-measurement procedures, and its absorbance was subtracted from the corresponding sample value before calculation. A glucose calibration curve was prepared over the range of 0–1.0 mg/mL, yielding the equation $A_{540} = 2.4786C - 0.0786$ ($R^2 = 0.9974$), where C represents the glucose-equivalent concentration in mg/mL. Undiluted culture supernatants were used only for preliminary comparative screening. For quantitative determination, the culture supernatants of the selected isolates and all subsequent samples were twofold serially diluted as required, and only dilutions yielding blank-corrected A_{540} values within the calibration range were used. One unit (U) was operationally defined as the amount of enzyme required to release 1 μg of glucose equivalents per minute under the specified assay conditions. Volumetric activity was calculated as follows:

$$\text{Endoglucanase activity}(\text{U/mL}) = (\triangle\text{C} \times \text{v} \times 1000 \times \text{D})/(\text{V} \times \text{t})$$

where ΔC is the glucose-equivalent concentration calculated from the blank-corrected absorbance using the calibration curve (mg/mL), v is the reaction volume before addition of DNS reagent (1.0 mL), V is the volume of crude extracellular enzyme preparation used

in the assay (0.5 mL), and t is the reaction time (30 min). D is the dilution factor, and 1000 converts milligrams to micrograms. The reported activity was back-calculated to that of the original undiluted culture supernatant using the corresponding dilution factor. For direct comparison with previous studies reporting enzyme activity in conventional international units, the mass-based activity values obtained in this study were additionally converted to IU using the relationship 1 IU = 180 of the units defined above. Three independently cultivated biological replicates were analyzed for each condition (n = 3).

2.3. Hemolysis Phenotype Assay

Single colonies of the selected isolates were spot-inoculated onto Columbia blood agar (Jiangmen Kailin Trading Co., Ltd., Jiangmen, China) and incubated at 37 °C for 24 h. *Staphylococcus aureus* served as a β-hemolytic positive control, whereas *Pseudomonas aeruginosa* was included as a reference strain. Hemolytic phenotypes were determined by visual examination of the zones surrounding the colonies: complete clearing was recorded as β-hemolysis, greenish discoloration as α-hemolysis, and the absence of visible changes as a non-hemolytic phenotype.

2.4. Growth Responses to Temperature Exposure and Initial pH

To characterize the ability of the selected isolates to resume growth after short-term exposure to different temperatures, as well as their growth responses to different initial pH conditions, bacterial suspensions were adjusted to an OD_{600} of 0.6, and 200 µL of each suspension was inoculated into 5 mL of Luria–Bertani (LB) broth. For the temperature-response assay, the inoculated cultures were exposed to 20, 30, 40, 50, 60, 70, or 80 °C in a water bath for 15 min. Immediately after exposure, all cultures were incubated at 37 °C and 180 rpm for 24 h, and endpoint growth was determined by measuring OD_{600}. Thus, this assay assessed relative growth recovery after short-term temperature exposure; it did not measure growth or extracellular enzyme production at the exposure temperatures. For the pH-response assay, the initial pH of LB broth was adjusted to 4.0, 5.0, 6.0, 7.0, 8.0, 9.0, or 10.0 using HCl or NaOH. Each pH-adjusted medium was inoculated with 200 µL of bacterial suspension adjusted to an OD_{600} of 0.6 and incubated at 37 °C and 180 rpm for 24 h before OD_{600} measurement. For the temperature series, the normalized metric was defined as relative post-exposure growth recovery, whereas for the pH series, it was defined as relative growth activity. Relative response (%) was calculated as follows: Relative response (%) = (OD_{600} of the treated condition/OD_{600} of the corresponding reference condition) × 100%. For each strain, the condition producing the highest mean OD_{600} within the corresponding temperature or pH series was used as the reference condition (100%). Three independently cultivated biological replicates were analyzed for each condition (n = 3).

2.5. Morphological and 16S rRNA-Based Characterization

Isolates were characterized by colony morphology, Gram staining, and 16S rRNA gene sequencing. Genomic DNA was extracted from pure cultures using a bacterial DNA isolation kit (Beijing Dingguo Changsheng Biotechnology Co., Ltd., Beijing, China) according to the manufacturer's instructions. The 16S rRNA gene was amplified with primers 27F (5′-AGAGTTTGATCCTGGCTCAG-3′) and 1492R (5′-TACGGCTACCTTGTTACGACTT-3′). PCR conditions were 95 °C for 3 min; 35 cycles of 95 °C for 30 s, 55 °C for 40 s, and 72 °C for 40 s; and 72 °C for 5 min. Products were separated on 1% agarose gels, purified, and bidirectionally sequenced. Taxonomic assignment was based on NCBI BLASTn (https://blast.ncbi.nlm.nih.gov/Blast.cgi?PROGRAM=blastn&PAGE_TYPE=BlastSearch, accessed on 13 October 2026, National Center for Biotechnology Information, Bethesda, MD, USA) similarity and phylogenetic placement, recognizing the limited species-level resolution of 16S rRNA within closely related *Bacillus* taxa [21]. Therefore, the isolates were con-

servatively referred to as *Bacillus* isolates H11 and Q5-3 throughout the manuscript. The sequences were deposited in GenBank as PZ702460 (H11) and PZ702461 (Q5-3).

2.6. Process-Variable Screening and Co-Culture Modeling

The liquid CMC-containing fermentation medium described above was used throughout the optimization experiments. Soluble CMC was selected as a standardized model substrate to provide a homogeneous and reproducible system for process-variable screening and co-culture optimization. After fixing the medium composition, the inoculum size, cultivation time, and initial pH were evaluated as operational variables affecting extracellular enzyme production.

Single-factor experiments were conducted using inoculum sizes of 1–16% (v/v), cultivation times of 12–72 h, and initial pH values of 4.0–9.0. When one variable was evaluated, the other conditions were maintained at an inoculum size of 1% (v/v), a cultivation time of 24 h, and an initial pH of 7.0. The tested pH range covered acidic, near-neutral, and alkaline conditions and was used to characterize the response profile of extracellular enzyme production. Extracellular endoglucanase, exoglucanase, and β-glucosidase activities were determined using clarified culture supernatants. Endoglucanase activity was measured as described above, whereas exoglucanase and β-glucosidase activities were determined according to Deshpande et al. [22] and Uchiyama et al. [23].

Based on the single-factor results, a three-factor, three-level L9(3^3) orthogonal array was used to optimize extracellular endoglucanase production by each isolate. Inoculum size, cultivation time, and initial pH were included as experimental factors, and extracellular endoglucanase activity was used as the response variable. The factor levels and experimental matrices are provided in Tables S2 and S3.

Co-culture conditions were subsequently optimized using a central composite design and response surface methodology in Design-Expert 13 (Stat-Ease, Inc., Minneapolis, MN, USA). Total inoculum volume and the Q5-3/H11 inoculum ratio (v/v) were used as independent variables, and extracellular endoglucanase activity in the clarified culture supernatant was used as the response. The predicted optimum was validated using three independently prepared biological replicates. The two-factor rotatable CCD comprised four factorial points, four axial points ($\alpha = \sqrt{2}$), and five center-point replicates (13 runs); the factor coding and complete design matrix are provided in Table S4.

2.7. Exploratory PCR Screening of Putative Endoglucanase-Related Targets

Fourteen primer pairs were used to screen genomic DNA from H11 and Q5-3 for cellulase-related targets. The selection of the target sequences and the design or compilation of the primer panel were informed by previously reported cellulase genes and primer sequences [24–26]. The target designations, primer sequences, and annealing temperatures used for each primer pair are provided in Table S1.

Genomic DNA from H11 and Q5-3 was used as the PCR template, and the primers were synthesized by Sangon Biotech (Shanghai) Co., Ltd., (Shanghai, China). Each 25 μL PCR mixture contained 12.5 μL of 2× Taq Plus Master Mix (Nanjing Vazyme Biotech Co., Ltd., Nanjing, China), 1 μL each of the forward and reverse primers (10 μmol/L), 1 μL of genomic DNA template, and nuclease-free water to a final volume of 25 μL. PCR amplification was performed using a gradient thermal cycler (Agilent Technologies, Inc., Santa Clara, CA, USA) with an initial denaturation at 95 °C for 3 min, followed by 35 cycles of denaturation at 95 °C for 30 s, annealing at the primer-specific temperature listed in Table S1 for 40 s, and extension at 72 °C for 40 s, with a final extension at 72 °C for 5 min. The amplification products were separated by agarose gel electrophoresis, visualized using a Bio-Rad gel documentation system (Bio-Rad Laboratories, Inc., Hercules, CA, USA) and

evaluated according to the presence of bands at the expected positions. The resulting amplification profiles were used for the preliminary comparison of cellulase-related targets between H11 and Q5-3.

2.8. Statistical Analysis

Quantitative experiments were conducted using three independently cultivated biological replicates for each condition (n = 3), and data are presented as the mean ± standard deviation (SD). The assumptions of normality and homogeneity of variance were assessed before parametric analysis. Differences among multiple groups were evaluated by one-way analysis of variance (ANOVA), followed by Dunnett's multiple-comparisons test, using GraphPad Prism 10.1.2 (GraphPad Software, Boston, MA, USA). Central composite design model fitting and the corresponding analysis of variance were performed using Design-Expert 13 (Stat-Ease, Inc., Minneapolis, MN, USA). Percentage changes were calculated from group means and rounded to the nearest integer. Model adequacy was evaluated using the complete ANOVA, lack-of-fit test, fit statistics, and residual and influence diagnostics provided in Tables S5–S8 and Figure S3.

3. Results

3.1. Screening of High Efficiency Cellulolytic Strains

A total of 86 CMC-hydrolyzing isolates were identified among the 180 gut-derived bacterial isolates from nine insect species. All positive isolates formed visible hydrolysis zones after Congo red staining. Figure 1A summarizes the numbers of total and CMC-hydrolyzing isolates recovered from *Lucilia sericata*, *Apis cerana*, *Locusta migratoria manilensis*, *Shirakiacris shirakii*, *Atractomorpha lata*, *Vespa affinis*, *Gryllus testaceus*, *Camponotus japonicus*, and *Atractomorpha sinensis*.

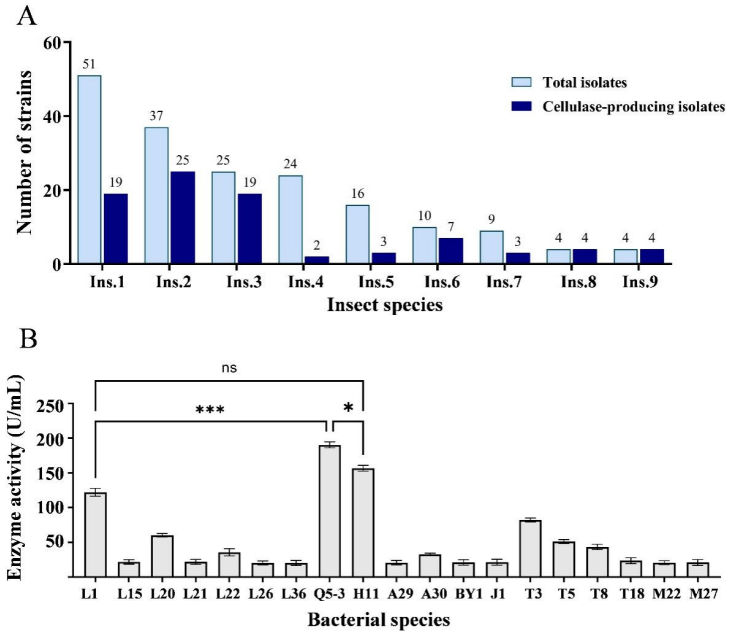


Figure 1. Screening of cellulase-producing strains from the gut microbiota of insects. (**A**) Distribution of gut bacterial isolates and cellulase producers among nine insect species, where Ins.1 to Ins.9 refers to nine insect species, respectively, as *Lucilia sericata*, *Apis cerana*, *Locusta migratoria manilensis*, *Shirakiacris shirakii*, *Atractomorpha lata*, *Vespa affinis*, *Gryllus testaceus*, *Camponotus japonicus*, and *Atractomorpha sinensis*. (**B**) Quantitative assessment of endoglucanase activity in strains exhibiting a high hydrolysis zone ratio (D/d > 3.0). Data are presented as the mean ± standard deviation (SD) of triplicate experiments (n = 3). Statistical significance between groups was determined by one-way ANOVA (*** $p < 0.001$, * $p < 0.05$, ns: not significant).

A total of 19 cellulase-producing strains, exhibiting high hydrolysis zone ratios ($D/d > 3.0$), were selected for the quantitative analysis of the extracellular endoglucanase activity using the DNS method, and the results are summarized in Figure 1B. The top three strains with the highest endoglucanase activities (>100 U/mL) were Q5-3 (190.36 ± 4.29 U/mL) from *A. sinensis*, H11 (156.67 ± 4.17 U/mL) from *S. shirakii*, and L1 (122.11 ± 5.65 U/mL) from *L. sericata*. These three strains were selected for subsequent investigation.

3.2. Biosafety Evaluation of the Cellulolytic Strains

Hemolytic phenotypes of L1, H11, and Q5-3 are shown in Figure 2. H11 and Q5-3 produced no visible hemolytic zones or greenish discoloration on Columbia blood agar, whereas L1 produced a clear zone consistent with β-hemolysis. Based on their non-hemolytic phenotypes, H11 and Q5-3 were retained for subsequent extracellular enzyme-production experiments. Further phenotypic and genomic safety assessments will be required before application-oriented evaluation of these isolates.

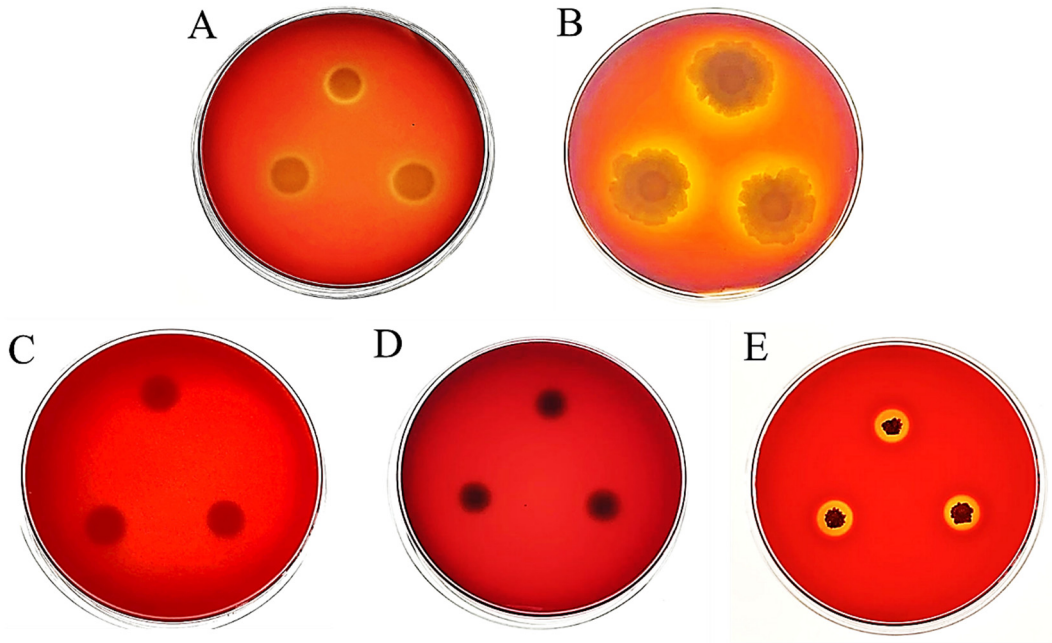


Figure 2. Hemolytic phenotypes of selected bacterial isolates and reference strains: (**A**) *Staphylococcus aureus*, β-hemolytic positive control; (**B**) *Pseudomonas aeruginosa*, pigment-producing reference strain showing greenish discoloration; (**C**) H11, with no visible hemolytic zone; (**D**) Q5-3, with no visible hemolytic zone; and (**E**) L1, showing a clear zone consistent with β-hemolysis. The colors shown represent the natural appearance of the blood agar plates and bacterial growth; no artificial color coding was used.

3.3. Responses to Temperature Exposure and Initial pH

Figure 3 shows the relative post-exposure growth recovery of H11 and Q5-3 after 15-min temperature treatments, together with their relative growth responses under different initial pH conditions. After exposure to different temperatures for 15 min and subsequent cultivation at 37 °C for 24 h, H11 showed relative post-exposure recovery values of approximately 90% following treatments at 20–50 °C, whereas lower recovery values were observed following exposure to 70 and 80 °C (Figure 3A). Under different initial pH conditions, H11 showed relative growth values of 71–83% across pH 5.0–9.0, with the highest value observed at pH 8.0; lower values were recorded at pH 4.0 and 10.0 (Figure 3B). Q5-3 showed post-exposure recovery values of 78–93% across the tested

temperature treatments, with the highest value observed following exposure to 50 °C (Figure 3C). Under different initial pH conditions, Q5-3 showed its highest relative growth values at pH 5.0–8.0, ranging from 78% to 92% (Figure 3D). Overall, both isolates showed post-exposure growth recovery across the tested temperature series, with Q5-3 exhibiting a more consistent response. Both isolates also maintained higher relative growth activity under intermediate initial pH conditions than under the extreme pH conditions tested.

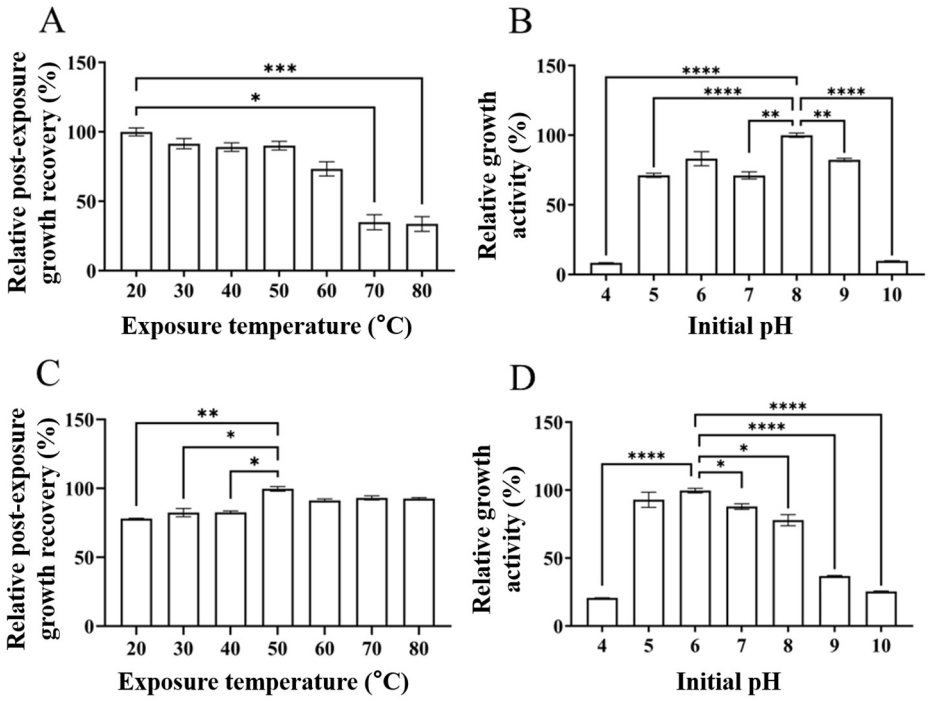


Figure 3. Post-exposure growth recovery and initial-pH responses of strains H11 and Q5-3. (**A**) Growth activity of H11 following temperature exposure. (**B**) Growth activity of H11 under different initial pH conditions. (**C**) Growth activity of Q5-3 following temperature exposure. (**D**) Growth activity of Q5-3 under different initial pH conditions. (**A**,**C**) Relative post-exposure growth recovery of H11 and Q5-3, respectively, following temperature exposure and subsequent cultivation at 37 °C. (**B**,**D**) Relative growth activity of H11 and Q5-3, respectively, under different initial pH conditions. Data are presented as the mean ± SD of three independent biological replicates (n = 3). Statistical significance relative to the designated reference condition in each panel was determined by one-way ANOVA, followed by Dunnett's multiple-comparisons test. **** $p < 0.0001$, *** $p < 0.001$, ** $p < 0.01$, and * $p < 0.05$. Only significant comparisons are indicated.

3.4. Morphological and 16S rRNA-Based Characterization of Isolates H11 and Q5-3

H11 and Q5-3 formed white, moist, smooth, convex colonies with irregular margins and were Gram-positive rods (Figure 4A,B). Their 16S rRNA gene sequences shared >99% identity with *Bacillus* sequences, and phylogenetic analysis placed both isolates closest to *B. subtilis* among the included references (Figure 4C). However, because 16S rRNA gene analysis alone does not provide sufficient resolution for reliable species-level identification among closely related *Bacillus* taxa, these results support assignment to the genus *Bacillus* but do not allow definitive identification as *B. subtilis*. Accordingly, the isolates are conservatively referred to as *Bacillus* isolates H11 and Q5-3 throughout the study. The GenBank accessions are PZ702460 for H11 and PZ702461 for Q5-3.

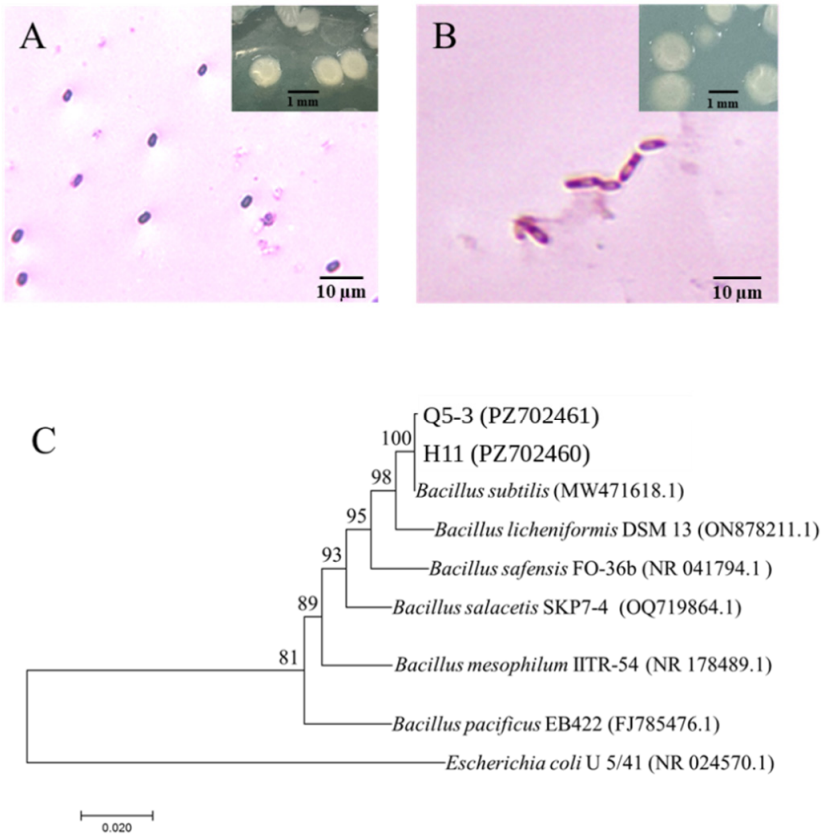


Figure 4. Morphology and 16S rRNA phylogeny of H11 and Q5-3. (**A**) Colony morphology and Gram staining of H11. (**B**) Colony morphology and Gram staining of Q5-3. (**C**) Phylogenetic tree based on 16S rRNA gene sequences, including H11 (PZ702460), Q5-3 (PZ702461), related *Bacillus* references, and *Escherichia coli* U 5/41 as the outgroup. Bootstrap values are based on 1000 replicates; values > 80% are shown. Scale bar, 0.020 substitutions per nucleotide position.

3.5. Extracellular Cellulase Activity Profiles of H11 and Q5-3

To characterize the extracellular cellulase activity profiles of H11 and Q5-3 under different cultivation conditions, endoglucanase, exoglucanase, and β-glucosidase activities were determined across a range of inoculum sizes, cultivation times, and initial pH values. For H11, the highest endoglucanase activities were observed at an inoculum size of 8% (*v*/*v*), a cultivation time of 36 h, and an initial pH of 6.0, respectively (Figure 5A–C). For Q5-3, maximum endoglucanase activities were obtained at an inoculum size of 4% (*v*/*v*), a cultivation time of 24 h, and an initial pH of 7.0, respectively (Figure S1). Across the tested cultivation conditions, endoglucanase activity showed a pronounced and consistent response in both isolates and remained comparatively high among the three extracellular cellulase activities examined. The crude enzyme preparations of H11 and Q5-3 therefore exhibited activity profiles characterized by prominent endoglucanase activity. Endoglucanases cleave internal β-1,4-glycosidic bonds within cellulose chains and generate additional chain ends that can facilitate subsequent exo-acting hydrolysis.

Accordingly, the activity profiles observed in this study indicate that both isolates exhibited pronounced CMC-hydrolyzing activity under the tested conditions. However, because the endoglucanase assessment relied on soluble CMC, these results do not demonstrate the hydrolysis or depolymerization of insoluble cellulose or lignocellulosic materials. Based on these results, volumetric endoglucanase activity in the culture supernatant (U/mL) was selected as the principal response variable for subsequent monoculture and co-culture process optimization.

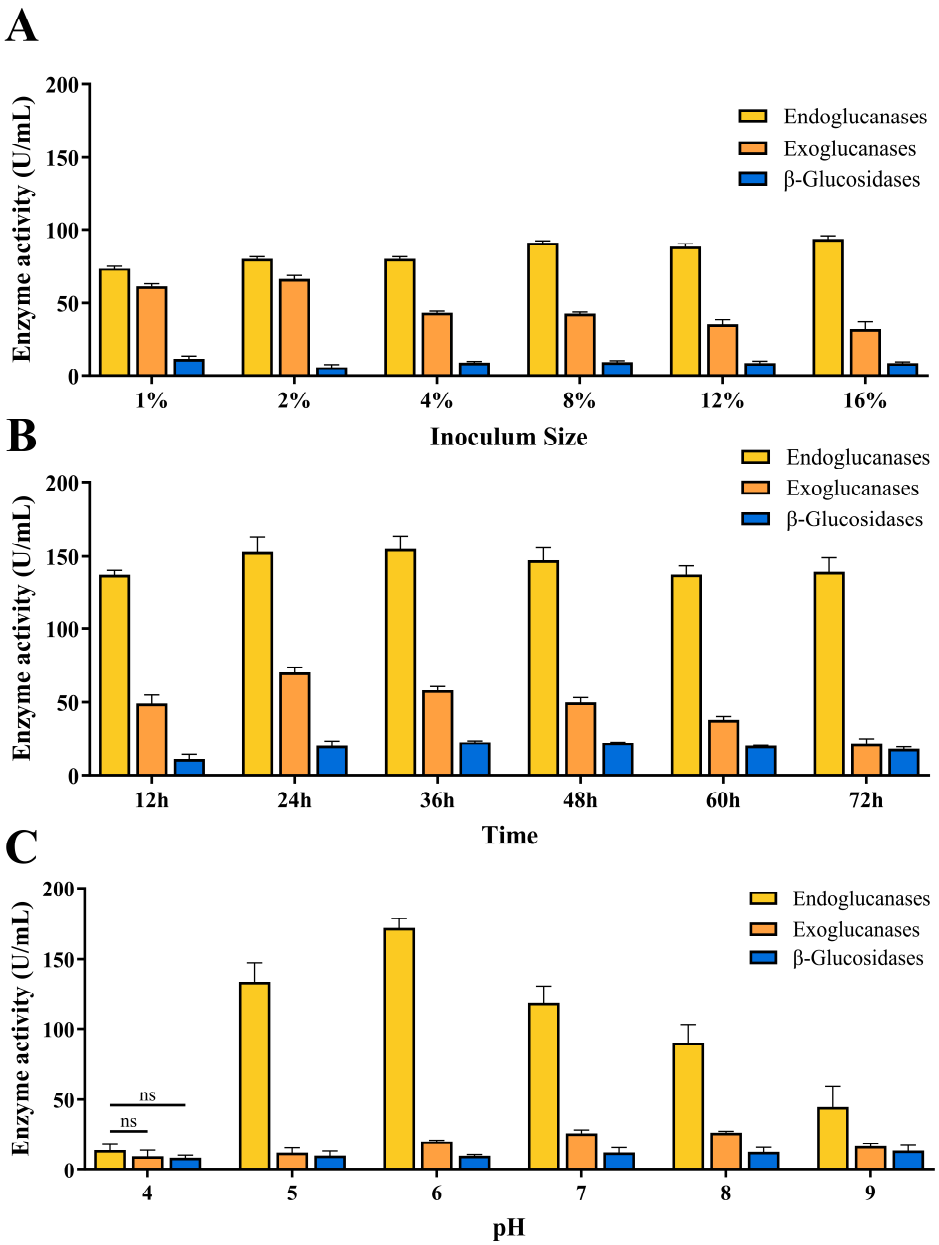


Figure 5. Effects of inoculum size, cultivation time, and initial pH on extracellular enzyme activities of H11. (**A**) Enzyme activities at different inoculum sizes. (**B**) Enzyme activities at different cultivation times. (**C**) Enzyme activities at different initial pH values. Values are mean ± SD (n = 3). Endoglucanase, exoglucanase, and β-glucosidase activities are expressed as U/mL of crude supernatant according to their respective assay definition. ns, not significant.

3.6. Orthogonal Optimization of Volumetric Extracellular Endoglucanase Activity

An L9(3^3) orthogonal array was used to optimize inoculum size, cultivation time, and initial pH after the single-factor experiments, with volumetric extracellular endoglucanase activity (U/mL) used as the endpoint response. The nine runs and range analyses for H11 and Q5-3 are provided in Tables S2 and S3. Range analysis identified initial pH as the largest contributor to variation in the volumetric activity response within the tested factor levels. The selected condition for both isolates was 8% inoculum, an initial of pH 5.0, and 24 h. Under this condition, the culture supernatants of H11 and Q5-3 showed volumetric extracellular endoglucanase activities of 228.01 ± 2.73 and 283.28 ± 2.06 U/mL endoglucanase, corresponding to increases of 46% and 49% relative to their respective pre-optimization values. These percentage increases describe changes in activity per unit culture-supernatant

volume and should not be interpreted as increases in enzyme production per unit biomass. The shared selected culture condition provided the basis for the subsequent two-strain co-culture optimization using the same volumetric activity response.

3.7. CCD Optimization of Co-Culture Conditions for Volumetric Extracellular Endoglucanase Activity

The quadratic model established using the central composite design was highly significant ($p < 0.0001$). The interaction between total inoculum volume and the Q5-3/H11 inoculum ratio (AB), as well as the quadratic effects of both variables (A^2 and B^2), significantly affected the modeled volumetric extracellular endoglucanase activity ($p < 0.05$). The model showed a strong fit to the experimental data, with an $R^2 = 0.9996$ and an adjusted $R^2 = 0.9993$, while the lack of fit was not significant ($p = 0.6048$). The complete design matrix and regression equations are provided in Table S4; coefficient estimates, ANOVA, and model-fit statistics are reported in Tables S5–S7; and run-level influence statistics and residual diagnostic plots are provided in Table S8 and Figure S3.

The response-surface and contour plots illustrate the combined effects of total inoculum volume and the Q5-3/H11 inoculum ratio on the volumetric activity response (Figure 6A,B). The model predicted the maximum volumetric response within the experimental design space at a total inoculum volume of 796.22 µL, corresponding to approximately 16% (*v*/*v*), and a Q5-3/H11 inoculum ratio of 2.08. Under these conditions, the predicted extracellular endoglucanase activity was 340.81 U/mL.

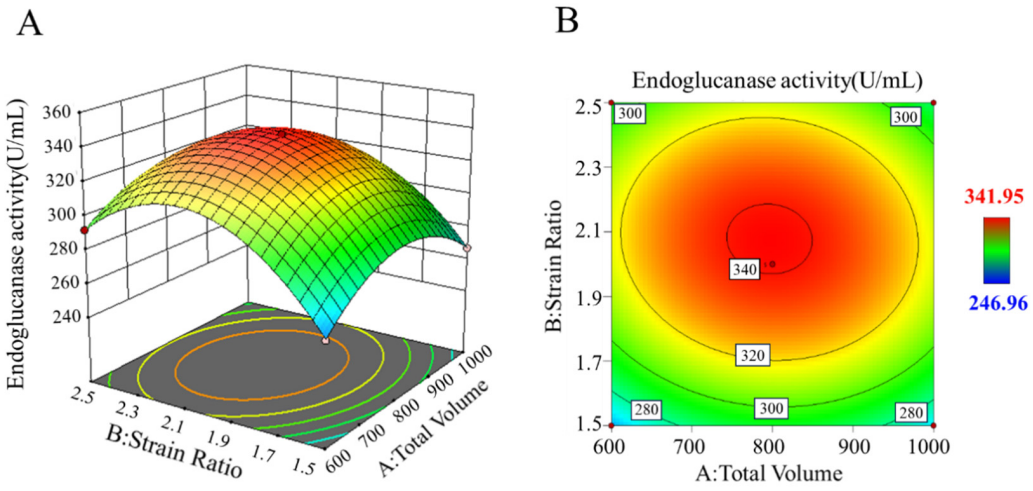


Figure 6. CCD response surfaces for volumetric extracellular endoglucanase activity in the H11–Q5-3 co-culture. (**A**) Three-dimensional response surface and (**B**) contour plot showing the modeled effects of total inoculum volume and the Q5-3/H11 inoculum ratio (*v*/*v*) on volumetric extracellular endoglucanase activity (U/mL). The red region indicates combinations predicted to yield higher activity within the experimental design space.

Experimental validation using three independently prepared co-cultures yielded a volumetric extracellular endoglucanase activity of 339.17 ± 3.97 U/mL, which closely agreed with the model-predicted value. To compare the monocultures and co-culture at the same total inoculum proportion, H11 and Q5-3 monocultures were additionally evaluated using approximately 16% inoculum under the same cultivation conditions as the validated co-culture. The matched H11 and Q5-3 monocultures yielded 96.69 ± 1.89 and 127.47 ± 7.24 U/mL, respectively, whereas the co-culture yielded 339.17 ± 3.97 U/mL. Thus, the co-culture showed 3.51- and 2.66-fold higher endpoint volumetric activities than the matched H11 and Q5-3 monocultures, corresponding to increases of approximately 251% and 166%, respectively (Figure 7). The activities previously obtained for H11 and

Q5-3 un-der the selected orthogonal monoculture condition—8% inoculum, an initial pH of 5.0, and 24 h—are included in Figure 7 only as reference values.

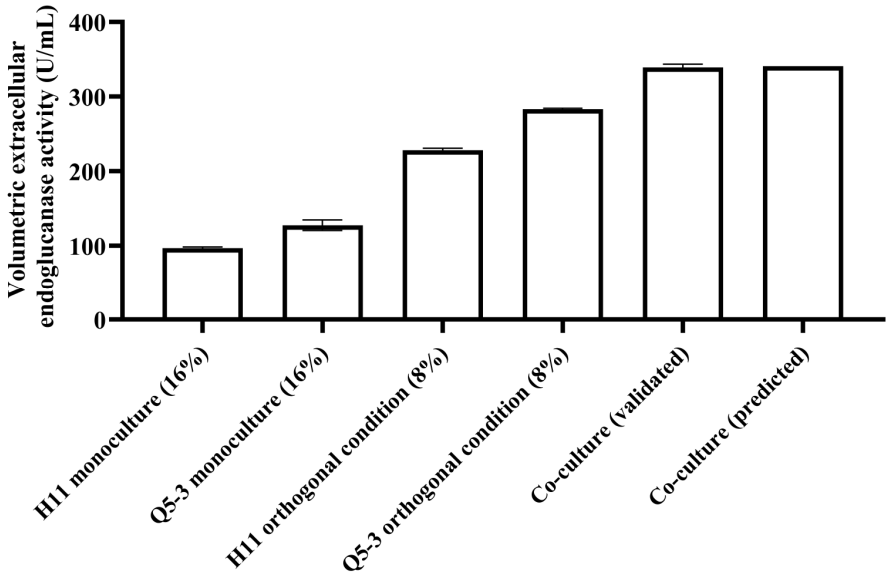


Figure 7. Comparison of volumetric extracellular endoglucanase activity under monoculture and co-culture conditions. H11 and Q5-3 monocultures containing 16% inoculum were evaluated under the same culture conditions as the validated H11–Q5-3 co-culture. Activities obtained under the selected orthogonal monoculture condition (8% inoculum, an initial pH of 5.0, and 24 h) are included for reference. Experimental data are presented as the mean ± SD of three independent biological replicates (n = 3). The CCD-predicted response (340.81 U/mL) is shown as an open symbol and was not included in the statistical analysis.

The CCD-predicted response is also shown in Figure 7 as a nonexperimental reference and was not included in the statistical comparisons. Because biomass at harvest was not determined, the matched-inoculum comparison is restricted to endpoint volumetric activity and does not establish increased enzyme production per unit biomass or a synergistic interaction between the two strains. However, because total inoculum proportion was held constant in this comparison, the higher co-culture endpoint cannot be attributed solely to the larger starting inoculum used in the original unmatched comparison. Overall, the close agreement between the predicted and experimentally validated co-culture responses supports the predictive performance of the CCD model within the tested soluble-CMC system.

3.8. PCR Amplification Profiles of Cellulase-Related Targets in H11 and Q5-3

Exploratory PCR screening using 14 primer pairs showed that five primer sets designed for the reported endoglucanase-related targets *egls*, *eg20SJ*, *Nqm*, *Cel5L*, and *eglsG* generated reproducible amplicons at the expected positions in both H11 and Q5-3 (Figure S2). The two isolates therefore showed similar PCR amplification profiles for these five primer sets. However, the amplicons were not sequenced, and gene expression or protein function was not evaluated. Therefore, these PCR products do not confirm the identities, expression, or functions of the intended targets and are not interpreted as molecular evidence for the observed endoglucanase phenotype. They are regarded only as preliminary candidate amplicons requiring sequence verification and functional analysis.

4. Discussion

In this study, two *Bacillus* isolates, H11 and Q5-3, with pronounced extracellular CMC-hydrolyzing activities were isolated from the guts of *Shirakiacris shirakii* and *Atractomorpha sinensis*, respectively. Plant-feeding insects are continuously exposed to cellulose-rich

plant materials, making their digestive tracts promising ecological sources for microorganisms and enzymes involved in plant-polysaccharide utilization [5,27]. Culture-dependent screening of grasshopper intestinal bacteria, including isolates obtained from *A. sinensis*, has likewise identified *Bacillus* strains capable of hydrolyzing carboxymethyl cellulose (CMC) [10]. The recovery of H11 and Q5-3 therefore reinforces the value of herbivorous insect guts as reservoirs for cellulolytic microbial resources and expands the range of insect-associated *Bacillus* isolates available for enzyme-production research. Although isolation from the gut does not alone establish the precise ecological roles of these bacteria in vivo, their measured CMC-hydrolyzing activities support further evaluation of this habitat as a source of candidate extracellular-enzyme-producing strains.

Both strains exhibited substantially higher apparent endoglucanase activity than exoglucanase and β-glucosidase activities under the tested conditions. This consistent pattern indicates that CMC-hydrolyzing activity was a prominent feature of the crude enzyme preparations produced by H11 and Q5-3. Endoglucanases cleave internal β-1,4-glycosidic bonds in cellulose chains, generating new chain ends and increasing substrate accessibility for subsequent hydrolysis by other cellulase components [28]. However, the present study evaluated endoglucanase activity using soluble CMC and did not assess the performance of the crude enzyme preparations against insoluble cellulose or in composite cellulase systems. Because the three activities were measured using different substrates and reaction conditions, their absolute values should be interpreted as profiles of detectable activity rather than as a precise quantitative description of the complete cellulase system. Nevertheless, the predominance of CMC-hydrolyzing activity in both strains supports their candidacy for further endoglucanase-focused investigation. CMC is widely used as a model substrate for endoglucanase assays [29]. Direct evaluation using insoluble cellulose and natural lignocellulosic substrates is therefore required before any relevance to biomass conversion can be assessed.

H11 and Q5-3 displayed distinct profiles of post-exposure growth recovery and responses to initial pH. H11 maintained relatively high growth activity across a broader range of initial pH values, whereas Q5-3 showed a more consistent post-exposure recovery profile across the tested temperature series. Although pH and temperature are important variables in microbial process development [30], the assays used here measured different responses: growth under different initial pH conditions and recovery following short-term temperature exposure. The observed differences in post-exposure recovery may motivate future investigation of strain-specific stress-response or protective systems [31]; these mechanisms were not examined in the present study. Both strains also showed a non-hemolytic phenotype under the conditions tested. This finding provides useful preliminary information for further strain development, while comprehensive application-oriented assessment will require additional phenotypic and genome-based evaluation. Despite their different post-exposure recovery and initial-pH response profiles, both isolates shared the same optimal cultivation settings among the variables examined: an inoculum level of 8%, an initial pH of 5.0, and a cultivation time of 24 h. This common condition provided a consistent basis for the subsequent co-culture modeling.

The identification of an intermediate optimal inoculum indicates that enzyme production was not simply proportional to the initial number of cells. Increasing the inoculum may shorten the lag phase and accelerate early substrate utilization, whereas an excessive inoculum may promote rapid nutrient depletion, oxygen limitation, metabolite accumulation, or an earlier transition to the stationary phase, thereby reducing final enzyme production. Previous studies have similarly shown that cellulase production by *Bacillus* is influenced by finite optima for inoculum size, pH, incubation time, and medium composition [32,33]. The 8% inoculum identified here may therefore represent a balance between rapid culture

establishment and maintenance of conditions favorable for extracellular enzyme accumulation. The 24 h optimum also indicates that both isolates produced substantial enzyme activity within a relatively short cultivation period, which may be favorable for fermentation productivity. The current optimization defines an effective operating window within the selected medium and tested ranges. Further adjustment of carbon and nitrogen sources, mineral supplementation, agitation, and oxygen transfer may provide additional gains, but the present conditions already established a consistent background for evaluating the effects of co-cultivation.

Under the validated co-culture condition, the endpoint volumetric extracellular endoglucanase activity reached 339.17 ± 3.97 U/mL (1.884 ± 0.022 IU/mL). When H11 and Q5-3 were cultivated separately at the same approximately 16% total inoculum proportion and under the same cultivation conditions, their corresponding activities were 96.69 ± 1.89 U/mL (0.537 ± 0.010 IU/mL) and 127.47 ± 7.24 U/mL (0.708 ± 0.040 IU/mL), respectively. Thus, the co-culture showed 3.51- and 2.66-fold higher endpoint volumetric activities than the matched H11 and Q5-3 monocultures, corresponding to increases of approximately 251% and 166%, respectively. Together, the matched-inoculum results show that the higher endpoint volumetric extracellular endoglucanase activity of the co-culture cannot be attributed solely to the larger total inoculum used in the original comparison, thereby supporting an association between co-cultivation and increased volumetric extracellular endoglucanase activity under the conditions tested in this study. Kazeem et al. [34] and Yang et al. [35] both reported enhanced cellulase activity in *Bacillus* co-culture systems relative to monocultures, consistent with the increase observed in the present study. This consistency across studies supports the general observation that co-cultivation of *Bacillus* strains can enhance cellulase production, although the magnitude of enhancement varies among systems, likely reflecting differences in bacterial strains, cultivation substrates, medium compositions, and enzyme assay conditions. In the present study, the central composite design showed that enzyme production depended on both total inoculum volume and the initial Q5-3/H11 ratio. The optimized ratio of 2.08 therefore represents a controllable process parameter rather than evidence that Q5-3 necessarily dominated the final population. More importantly, the existence of a defined optimum indicates that the co-culture response was not produced merely by mixing two strains but was associated with the initial balance between them.

Several non-exclusive mechanisms may explain the enhanced production observed in the co-culture. H11 and Q5-3 may secrete partially complementary enzymes or accessory proteins, resulting in a combined extracellular preparation with greater activity than either monoculture preparation [36,37]. Functional complementation among community members has been demonstrated in cellulose-degrading consortia, in which different microorganisms contributed distinct carbohydrate-active enzymes and metabolic functions [38]. Metabolites released by one strain may also support the growth or enzyme production of the other through cross-feeding interactions [39], while one strain may modify extracellular pH, nutrient availability, or inhibitory hydrolysis-product concentrations in a manner favorable to the other. Quorum-sensing systems are known to coordinate population-level behaviors and extracellular-product formation in bacteria [40], and regulatory links between bacterial signaling and carbohydrate-active enzymes have been reported in specific microbial systems [41]. The occurrence of a defined optimum at an initial Q5-3/H11 ratio of 2.08 suggests that the co-culture response was composition-dependent. This observation is consistent with enzyme complementation, cross-feeding, environmental modification, or density-dependent signaling, as these processes may require an appropriate balance between the two strains. However, because strain-specific biomass and the final population ratio were not measured, this result does not distinguish among these

mechanisms or demonstrate that Q5-3 dominated the population at harvest. Strain-specific population measurements, metabolite profiling, secretome analysis, and transcriptional studies would clarify whether the enhancement is driven primarily by enzyme complementation, metabolic exchange, environmental modification, or regulatory signaling. The current results are limited to volumetric enzyme activity determined using soluble CMC. They do not establish the hydrolysis or saccharification of insoluble cellulose or agricultural residues. Substrate conversion, saccharification yield, and fermentable-sugar release must be evaluated directly in future studies.

PCR screening provided an additional molecular perspective on the cellulolytic potential of H11 and Q5-3. Primer pairs targeting the reported endoglucanase-related sequences *egls*, *eg20SJ*, *Nqm*, *Cel5L*, and *eglsG* generated amplicons of the expected sizes in both isolates. The target selection was based on previously reported endoglucanases with potentially valuable catalytic characteristics. Acid-active or acid-tolerant enzymes related to some of these targets have been described [42], whereas other reported enzymes display thermostability or activity across broad temperature ranges [43]. These studies support the relevance of the selected regions as candidates for molecular screening. Because the amplicons have not yet been sequenced, they are most appropriately described as putative endoglucanase-related fragments rather than confirmed functional genes. Even so, the PCR results provide a focused set of targets for subsequent sequencing, genome annotation, and functional analysis. The similar amplification patterns of H11 and Q5-3, together with their distinct post-exposure growth-recovery, initial-pH response, and enzyme-production profiles, further suggest that phenotypic variation may depend not only on the presence of cellulase-related sequences but also on their regulation, expression, and secretion. Cellulolytic performance is shaped by the coordinated expression of carbohydrate-active enzymes and associated regulatory pathways [44,45]. Future sequence and expression analyses may therefore reveal how the two strains generate distinct phenotypic and enzyme-production characteristics despite sharing similar candidate target profiles.

Taken together, the present study establishes a process-development framework for extracellular endoglucanase production using the insect-gut-derived Bacillus isolates H11 and Q5-3. By integrating strain screening, monoculture optimization, co-culture modeling, experimental validation, and matched-inoculum controls, the study defines a reproducible basis for evaluating co-cultivation performance in a controlled soluble-CMC system. In particular, the matched-inoculum comparison strengthens the process-level interpretation by showing that the higher endpoint volumetric activity of the co-culture was maintained after controlling for total initial inoculum. The initial strain ratio identified by the CCD therefore provides a practical process parameter for defining and optimizing the co-culture composition. Overall, these results support H11 and Q5-3 as candidate production strains and establish a defined co-cultivation condition for further development of extracellular endoglucanase production.

The process framework established here also provides a clear basis for extending this co-culture system toward broader biochemical and application-oriented evaluation. Further work can examine strain-resolved population dynamics, extracellular protein profiles, metabolite exchange, and gene expression to determine how the two isolates contribute to the enhanced co-culture phenotype. In parallel, the characterization of the extracellular enzyme preparations across different substrates, pH values, and temperatures will help to define their catalytic properties and operational stability. Evaluation with insoluble cellulose and representative lignocellulosic feedstocks can then determine how effectively the optimized soluble-CMC process translates to structurally more complex substrates, including its effects on reducing-sugar release, substrate conversion, and saccharification efficiency. These successive levels of analysis will build on the present process-development

results and clarify the potential of H11 and Q5-3 for future cellulase production and cellulose-rich biomass bioconversion.

Supplementary Materials: The following supporting information can be downloaded at https://www.mdpi.com/article/10.3390/fermentation12100482/s1, Table S1: Primer sequences used for exploratory PCR screening of putative cellulase-related targets; Table S2: L9(3^3) orthogonal design matrix and measured extracellular endoglucanase activities of strains H11 and Q5-3; Table S3: Range analysis of factor effects on extracellular endoglucanase activity in strains H11 and Q5-3; Table S4: Complete central composite design matrix and model predictions; Table S5: Coefficient estimates for the quadratic model in coded factors; Table S6: Analysis of variance for the fitted quadratic model; Table S7: Model fit statistics; Table S8: Run-level residual and influence diagnostics; Figure S1: Effects of inoculum size, cultivation time and pH on the activities of endoglucanase, exoglucanase, and β-glucosidase in strain Q5-3; Figure S2: Exploratory PCR amplification of putative endoglucanase-related targets in H11 and Q5-3; Figure S3: Diagnostic plots for the fitted quadratic CCD model.

Author Contributions: Conceptualization, F.C. and X.Y.; methodology, W.X., X.J. and S.L.; investigation, L.F.; formal analysis, W.X., L.F., X.J. and S.L.; data curation, W.X., L.F., X.J. and S.L.; validation, W.X., F.C., X.J. and S.L.; visualization, L.F.; writing—original draft preparation, L.F.; writing—review and editing, W.X., F.C. and X.Y.; supervision, F.C.; funding acquisition, F.C. and X.Y. All authors have read and agreed to the published version of the manuscript.

Funding: This work was supported by the National Natural Science Foundation of China [Grant No. 42177406] and the Natural Science Foundation of Liaoning Province [Grant No. 2023-MS-319].

Institutional Review Board Statement: This study complied with all relevant international and local ethical guidelines for scientific research. No endangered or protected species, human participants, or human biological samples were involved in the work. All experimental operations followed the principles of humane treatment of research organisms, and no additional ethical approval was required for this study.

Informed Consent Statement: Not applicable.

Data Availability Statement: The data underlying this article are available in the article and in its online Supplementary Materials.

Acknowledgments: The authors thank all members of Fangmin Chen's research group for their valuable comments on and suggestions regarding this work.

Conflicts of Interest: The authors declare no conflict of interest.

References

1. Stork, N.E. How many species of insects and other terrestrial arthropods are there on Earth? *Annu. Rev. Entomol.* **2018**, *63*, 31–45. [CrossRef] [PubMed]
2. Watanabe, H.; Tokuda, G. Cellulolytic systems in insects. *Annu. Rev. Entomol.* **2010**, *55*, 609–632. [CrossRef] [PubMed]
3. Shamjana, U.; Vasu, D.A.; Hembrom, P.S.; Nayak, K.; Grace, T. The role of insect gut microbiota in host fitness, detoxification and nutrient supplementation. *Antonie Van Leeuwenhoek* **2024**, *117*, 71. [CrossRef] [PubMed]
4. Liu, T.; Sun, Z.; Yang, Z.; Qiao, X. Microbiota-derived short-chain fatty acids and modulation of host-derived peptide formation: Focused on host defense peptides. *Biomed. Pharmacother.* **2023**, *162*, 114586. [CrossRef] [PubMed]
5. Su, L.J.; Liu, H.; Li, Y.; Zhang, H.F.; Chen, M.; Gao, X.H.; Wang, F.Q.; Song, A.D. Cellulolytic activity and structure of symbiotic bacteria in locust guts. *Genet. Mol. Res.* **2014**, *13*, 7926–7936. [CrossRef] [PubMed]
6. Huang, J.; Weng, L.; Zhang, X.; Long, K.; An, X.; Bao, J.; Wu, H.; Zhou, X.; Zhang, S. *Trypoxylus dichotomus* gut bacteria provides an effective system for bamboo lignocellulose degradation. *Microbiol. Spectr.* **2022**, *10*, e02147-22. [CrossRef] [PubMed]
7. Dar, M.A.; Shaikh, A.F.; Pawar, K.D.; Xie, R.; Sun, J.; Kandasamy, S.; Pandit, R.S. Evaluation of cellulose-degrading bacteria isolated from the gut-system of cotton bollworm, *Helicoverpa armigera*, and their potential values in biomass conversion. *PeerJ* **2021**, *9*, e11254. [CrossRef] [PubMed]

8. Azhar, S.; Aihetasham, A.; Chaudhary, A.; Hussain, Z.; Abdul Rehman, R.; Abbas, G.; Alharbi, S.A.; Ansari, M.J.; Qamer, S. Cellulolytic and ethanologenic evaluation of *Heterotermes indicola*'s gut-associated bacterial isolates. *ACS Omega* **2024**, *9*, 12084–12100. [CrossRef] [PubMed]
9. Kumawat, P.K.; Sarkar, S.; Kumar, S.; Sahoo, A. Lower termite (*Coptotermes heimi*) gut fibrolytic bacterial consortium: Isolation, phylogenetic characterization, fibre degradation potential and in vitro digestibility. *PLoS ONE* **2025**, *20*, e0318090. [CrossRef] [PubMed]
10. Li, W.J.; Li, F.F.; Bai, J.; Liang, K.; Li, K.; Qin, G.Q.; Zhang, Y.L.; Li, X.J. Isolation and characterization of intestinal bacteria associated with cellulose degradation in grasshoppers (Orthoptera). *J. Insect Sci.* **2023**, *23*, 7. [CrossRef] [PubMed]
11. Su, R.R.; Pan, B.Q.; Luo, Y.X.; Zheng, X.L.; Lu, W.; Wang, X.Y. Characterization of bacterial diversity and screening of cellulose-degrading bacteria in the gut system of *Glenea cantor* (Fabricius) larvae. *Front. Bioeng. Biotechnol.* **2024**, *12*, 1340168. [CrossRef] [PubMed]
12. Vishnu Vyasa, G.; Narasingappa, R.B.; Prakash, K.V.; Bhavani, P.; Gagandeep, K.R. Prospecting cellulolytic bacteria from white grubs (*Holotrichia serrata* (F.) and *Leucopholis coneophora* Burmeister) native to the Karnataka region. *BMC Microbiol.* **2025**, *25*, 121. [CrossRef] [PubMed]
13. Gales, A.; Chatellard, L.; Abadie, M.; Bonnafous, A.; Auer, L.; Carrère, H.; Godon, J.J.; Hernandez-Raquet, G.; Dumas, C. Screening of phytophagous and xylophagous insect gut microbiota abilities to degrade lignocellulose in bioreactor. *Front. Microbiol.* **2018**, *9*, 2222. [CrossRef] [PubMed]
14. Ire, F.S.; Ezebuiro, V.; Ogugbue, C.J. Production of bioethanol by bacterial co-culture from agro-waste-impacted soil through simultaneous saccharification and co-fermentation of steam-exploded bagasse. *Bioresour. Bioprocess.* **2016**, *3*, 26. [CrossRef]
15. Asiri, M.; Singh, T.; Mohammad, A.; Al Ali, A.; Alqahtani, A.; Saeed, M.; Srivastava, M. Bacterial cellulase production via co-fermentation of paddy straw and litchi waste and its stability assessment in the presence of Zn–Mg mixed-phase hydroxide-based nanocomposite derived from Litchi chinensis seeds. *Int. J. Biol. Macromol.* **2023**, *238*, 124284. [CrossRef] [PubMed]
16. Soares, J.F.; Confortin, T.C.; Todero, I.; Mayer, F.D.; Mazutti, M.A. Dark fermentative biohydrogen production from lignocellulosic biomass: Technological challenges and future prospects. *Renew. Sustain. Energy Rev.* **2020**, *117*, 109484. [CrossRef]
17. Periyasamy, S.; Karthik, V.; Senthil Kumar, P.; Isabel, J.B.; Temesgen, T.; Hunegnaw, B.M.; Melese, B.B.; Mohamed, B.A.; Vo, D.V.N. Chemical, physical and biological methods to convert lignocellulosic waste into value-added products: A review. *Environ. Chem. Lett.* **2022**, *20*, 1129–1152. [CrossRef]
18. Kuhad, R.C.; Gupta, R.; Singh, A. Microbial cellulases and their industrial applications. *Enzym. Res.* **2011**, *2011*, 280696. [CrossRef] [PubMed]
19. Sukharnikov, L.O.; Cantwell, B.J.; Podar, M.; Zhulin, I.B. Cellulases: Ambiguous nonhomologous enzymes in a genomic perspective. *Trends Biotechnol.* **2011**, *29*, 473–479. [CrossRef] [PubMed]
20. McKee, L.S. Measuring enzyme kinetics of glycoside hydrolases using the 3,5-dinitrosalicylic acid assay. *Methods Mol. Biol.* **2017**, *1588*, 27–36. [CrossRef] [PubMed]
21. Kim, M.; Oh, H.S.; Park, S.C.; Chun, J. Towards a taxonomic coherence between average nucleotide identity and 16S rRNA gene sequence similarity for species demarcation of prokaryotes. *Int. J. Syst. Evol. Microbiol.* **2014**, *64*, 346–351. [CrossRef] [PubMed]
22. Deshpande, M.V.; Eriksson, K.E.; Pettersson, L.G. An assay for selective determination of exo-1,4-beta-glucanases in a mixture of cellulolytic enzymes. *Anal. Biochem.* **1984**, *138*, 481–487. [CrossRef] [PubMed]
23. Uchiyama, T.; Yaoi, K.; Miyazaki, K. Glucose-tolerant β-glucosidase retrieved from a Kusaya gravy metagenome. *Front. Microbiol.* **2015**, *6*, 548. Correction in *Front. Microbiol.* **2015**, *6*, 1131. https://doi.org/10.3389/fmicb.2015.01131. [CrossRef] [PubMed]
24. El-Khamisi, E.F.; Soliman, E.A.M.; El-Sayed, G.M.; Nour, S.A.; Abdel-Monem, M.O.; Hassan, M.G. Optimization, gene cloning, expression, and molecular docking insights for enhanced cellulase enzyme production by *Bacillus amyloliquefaciens* strain elh1. *Microb. Cell Fact.* **2024**, *23*, 191. [CrossRef] [PubMed]
25. Kim, D.; Ku, S. *Bacillus* cellulase molecular cloning, expression, and surface display on the outer membrane of *Escherichia coli*. *Molecules* **2018**, *23*, 503. [CrossRef] [PubMed]
26. Zeng, X.; Ren, X.; Wu, R.; Zhang, Y.; Zhang, C.; Ran, S.; Ma, L. Screening, gene cloning and expression of cellulase-producing strain *Bacillus subtilis* Xh-16. *Curr. Microbiol.* **2024**, *81*, 452. [CrossRef] [PubMed]
27. Shelomi, M.; Heckel, D.G.; Pauchet, Y. Ancestral gene duplication enabled the evolution of multifunctional cellulases in stick insects (Phasmatodea). *Insect Biochem. Mol. Biol.* **2016**, *71*, 1–11. [CrossRef] [PubMed]
28. Tambor, J.H.; Ren, H.; Ushinsky, S.; Zheng, Y.; Riemens, A.; St-Francois, C.; Tsang, A.; Powlowski, J.; Storms, R. Recombinant expression, activity screening and functional characterization identifies three novel endo-1,4-β-glucanases that efficiently hydrolyse cellulosic substrates. *Appl. Microbiol. Biotechnol.* **2012**, *93*, 203–214. [CrossRef] [PubMed]
29. Xiao, Z.; Storms, R.; Tsang, A. Microplate-based carboxymethylcellulose assay for endoglucanase activity. *Anal. Biochem.* **2005**, *342*, 176–178. [CrossRef] [PubMed]
30. Olsson, L.; Rugbjerg, P.; Torello Pianale, L.; Trivellin, C. Robustness: Linking strain design to viable bioprocesses. *Trends Biotechnol.* **2022**, *40*, 918–931. [CrossRef] [PubMed]

31. Linton, S.M. Review: The structure and function of cellulase (endo-β-1,4-glucanase) and hemicellulase (β-1,3-glucanase and endo-β-1,4-mannase) enzymes in invertebrates that consume materials ranging from microbes and algae to leaf litter. *Comp. Biochem. Physiol. Part B Biochem. Mol. Biol.* **2020**, *240*, 110354. [CrossRef] [PubMed]
32. Deka, D.; Das, S.P.; Sahoo, N.; Das, D.; Jawed, M.; Goyal, D.; Goyal, A. Enhanced cellulase production from *Bacillus subtilis* by optimizing physical parameters for bioethanol production. *ISRN Biotechnol.* **2013**, *2013*, 965310. [CrossRef] [PubMed]
33. Nair, A.S.; Al-Battashi, H.; Al-Akzawi, A.; Annamalai, N.; Gujarathi, A.; Al-Bahry, S.; Dhillon, G.S.; Sivakumar, N. Waste office paper: A potential feedstock for cellulase production by a novel strain *Bacillus velezensis* ASN1. *Waste Manag.* **2018**, *79*, 491–500. [CrossRef] [PubMed]
34. Kazeem, M.O.; Ajijolakewu, K.A.; Abdul Rahman, N.A. Cellulase production by co-culture of *Bacillus licheniformis* and *Bacillus paralicheniformis* over monocultures on microcrystalline cellulose and chicken manure-supplemented rice bran media. *BioResources* **2021**, *16*, 6850–6869. [CrossRef]
35. Yang, G.; Yang, D.; Wang, X.; Cao, W. A novel thermostable cellulase-producing *Bacillus licheniformis* A5 acts synergistically with *Bacillus subtilis* B2 to improve degradation of Chinese distillers' grains. *Bioresour. Technol.* **2021**, *325*, 124729. [CrossRef] [PubMed]
36. Zhang, K.; Chen, X.; Schwarz, W.H.; Li, F. Synergism of glycoside hydrolase secretomes from two thermophilic bacteria cocultivated on lignocellulose. *Appl. Environ. Microbiol.* **2014**, *80*, 2592–2601. [CrossRef] [PubMed]
37. Zhao, W.; Wu, Y.; Fu, C.; Li, L. Mutualistic cross-feeding mediated by metabolic intermediates and siderophores enhances dibenzo-p-dioxin removal. *Environ. Sci. Technol.* **2025**, *59*, 14508–14517. [CrossRef] [PubMed]
38. Zhou, Y.; Pope, P.B.; Li, S.; Wen, B.; Tan, F.; Cheng, S.; Chen, J.; Yang, J.; Liu, F.; Lei, X.; et al. Omics-based interpretation of synergism in a soil-derived cellulose-degrading microbial community. *Sci. Rep.* **2014**, *4*, 5288. [CrossRef] [PubMed]
39. D'Souza, G.; Shitut, S.; Preussger, D.; Yousif, G.; Waschina, S.; Kost, C. Ecology and evolution of metabolic cross-feeding interactions in bacteria. *Nat. Prod. Rep.* **2018**, *35*, 455–488. [CrossRef] [PubMed]
40. Williams, P.; Winzer, K.; Chan, W.C.; Cámara, M. Look who's talking: Communication and quorum sensing in the bacterial world. *Philos. Trans. R. Soc. Lond. B Biol. Sci.* **2007**, *362*, 1119–1134. [CrossRef] [PubMed]
41. Senuma, W.; Tsuzuki, M.; Takemura, C.; Terazawa, Y.; Inoue, K.; Kiba, A.; Ohnishi, K.; Kai, K.; Hikichi, Y. β-1,4-Cellobiohydrolase is involved in full expression of phcA, contributing to the feedback loop in quorum sensing of Ralstonia pseudosolanacearum strain OE1-1. *Mol. Plant Pathol.* **2023**, *24*, 549–559. [CrossRef] [PubMed]
42. Joshi, N.; Kaushal, G.; Singh, S.P. Biochemical characterization of a novel thermo-halo-tolerant GH5 endoglucanase from a thermal spring metagenome. *Biotechnol. Bioeng.* **2021**, *118*, 1531–1544. [CrossRef] [PubMed]
43. Okano, H.; Kanaya, E.; Ozaki, M.; Angkawidjaja, C.; Kanaya, S. Structure, activity, and stability of metagenome-derived glycoside hydrolase family 9 endoglucanase with an N-terminal Ig-like domain. *Protein Sci.* **2015**, *24*, 408–419. [CrossRef] [PubMed]
44. Wohlbach, D.J.; Rovinskiy, N.; Lewis, J.A.; Sardi, M.; Schackwitz, W.S.; Martin, J.A.; Deshpande, S.; Daum, C.G.; Lipzen, A.; Sato, T.K.; et al. Comparative genomics of Saccharomyces cerevisiae natural isolates for bioenergy production. *Genome Biol. Evol.* **2014**, *6*, 2557–2566. [CrossRef] [PubMed]
45. Lamour, J.; Wan, C.; Zhang, M.; Zhao, X.; den Haan, R. Overexpression of endogenous stress-tolerance-related genes in Saccharomyces cerevisiae improved strain robustness and production of heterologous cellobiohydrolase. *FEMS Yeast Res.* **2019**, *19*, foz035. [CrossRef] [PubMed]

Disclaimer/Publisher's Note: The statements, opinions and data contained in all publications are solely those of the individual author(s) and contributor(s) and not of MDPI and/or the editor(s). MDPI and/or the editor(s) disclaim responsibility for any injury to people or property resulting from any ideas, methods, instructions or products referred to in the content.